

A two-tier monolithically stacked CMOS Active Pixel Sensor to measure charged particle direction

This content has been downloaded from IOPscience. Please scroll down to see the full text.

2014 JINST 9 C05038

(<http://iopscience.iop.org/1748-0221/9/05/C05038>)

View [the table of contents for this issue](#), or go to the [journal homepage](#) for more

Download details:

IP Address: 137.138.125.163

This content was downloaded on 08/07/2014 at 08:15

Please note that [terms and conditions apply](#).

15th INTERNATIONAL WORKSHOP ON RADIATION IMAGING DETECTORS
23–27 JUNE 2013,
PARIS, FRANCE

A two-tier monolithically stacked CMOS Active Pixel Sensor to measure charged particle direction

D. Passeri,^{a,b,1} L. Servoli,^b S. Meroli,^c D. Magalotti,^d P. Placidi^{a,b} and A. Marras^e

^aDipartimento di Ingegneria Elettronica e Informazione, Università di Perugia,
via G. Duranti 93, Perugia, Italy

^bIstituto Nazionale Fisica Nucleare — Sezione di Perugia,
via A. Pascoli 1, Perugia, Italy

^cCERN,
CH-1211 Geneva 23, Switzerland

^dDipartimento di Ingegneria, Università di Modena,
Strada Vignolese 905 - 41125 Modena, Italy

^eDESY Deutsches Elektronen-Synchrotron,
Hamburg, Germany

E-mail: daniele.passeri@unipg.it

ABSTRACT: In this work we present an innovative approach to particle tracking based on CMOS Active Pixel Sensors (APS) layers, monolithically integrated in an all-in-one chip featuring multiple, stacked, fully functional detector layers capable to provide momentum measurement (particle direction) within a single detector by using multiple layer impact point coordinates. The whole system will result in a very low material detector, since each layer can be thinned down to tens of micrometres, thus dramatically reducing multiple scattering issues. To build such a detector, we rely on the capabilities of the CMOS vertical scale integration (3D-IC) 130 nm Chartered/Tezzaron technology, used to integrate two fully-functional CMOS APS matrix detectors, including both sensing area and control/signal elaboration circuitry, stacked in a monolithic device by means of Through Silicon Via (TSV) connections. Such a detector would allow accurate estimation of the impact point of an ionizing particle and of its incidence angle. Two batches of the first chip prototype have been produced and characterized using particle beams (e.g. protons) demonstrating the suitability of particle direction measurement with a single, multiple layers, 3D vertically stacked APS CMOS detector.

KEYWORDS: Particle tracking detectors (Solid-state detectors); VLSI circuits

¹Corresponding author.

Contents

1	Introduction	1
1.1	The two-tier 3D monolithically stacked CMOS Active Pixel Sensors	2
2	System characterization	3
2.1	Electrical characterization	3
2.2	Calibration	4
3	Characterization with protons: angular measurements	6
4	Conclusions	9

1 Introduction

Typical tracking systems for particle trajectory reconstruction in High Energy Physics experiments are usually based on different separated sensing layers, featuring pixels and/or strips elements. In this work we present the results of the characterization of an innovative particle tracking detector, based on CMOS Active Pixel Sensors (APS) layers, monolithically integrated in an all-in-one chip featuring multiple stacked detector layers capable to provide momentum measurement (particle impact point and direction) within a single detector. This approach will result in a very low material detector, thus reducing multiple scattering issues, e.g. the error induced on the track reconstruction due to particle interaction with matter, since each layer can be thinned down to tens of micrometres.

To build such a detector, we rely on the capabilities of the CMOS vertical scale integration (3D-IC) 130 nm Chartered (now GlobalFoundries)/Tezzaron technology, used to integrate two fully-functional CMOS APS matrix detectors, including both sensing area and control/signal elaboration circuitry, stacked in a monolithic device by means of Through Silicon Via (TSV) connections. Such a detector would allow accurate estimation of the impact point of an ionizing particle (with intrinsic spatial resolution in the micrometre range) and of its incidence angle (with angular precision around 1°) [1]. The first batch of chip prototypes has been recently delivered and characterized in terms of noise and charge to signal conversion gain in laboratory using a variety of ionizing radiation sources (laser, X-rays) [2].

In this work we report on the first extensive characterization of a second batch of chip prototypes carried out using particle beams (protons of different energies) as well as on the perspective of this new approach for angular measurement of a particle trajectory. It is worthwhile to notice that other groups are currently designing and implementing some solid state momentum measurement device, usually with a much longer lever arm, e.g. in view of the challenge of using the tracker information at Level 1 trigger at future High Luminosity Large Hadron Collider at CERN [3]. Our approach could significantly reduce the problem of the treatment of information coming from different layers of these devices, and of the hardware implementation of coincidence logics at a level very close to the signal formation.

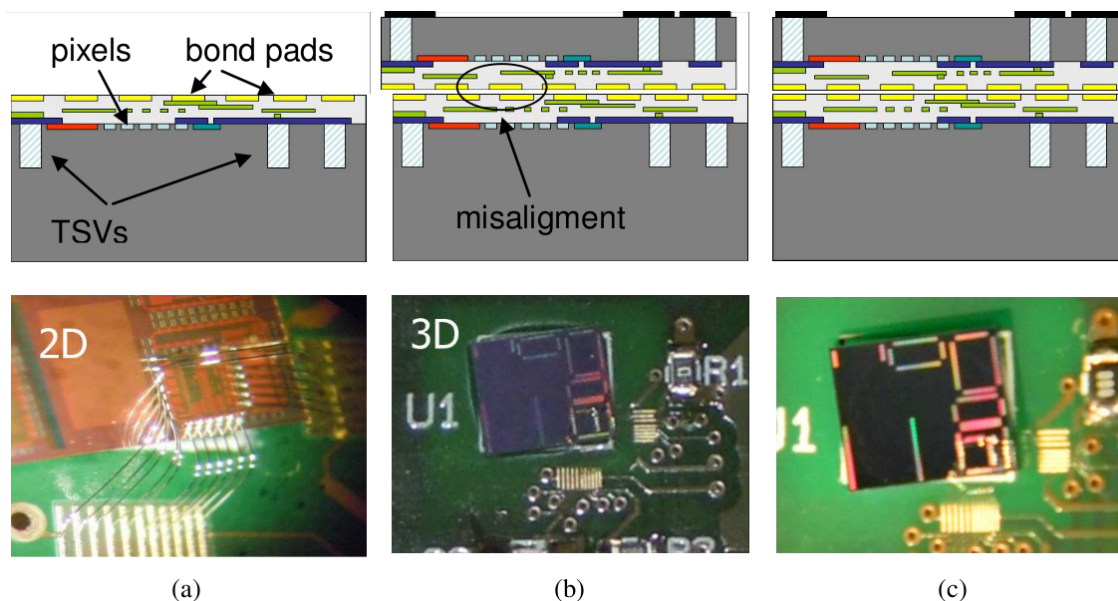


Figure 1. Schematic cross-sections and micro-photographs of the different structures: (a) 2D, (b) 3D not aligned, (c) 3D aligned.

1.1 The two-tier 3D monolithically stacked CMOS Active Pixel Sensors

Different chip prototypes have been fabricated within a multi-project run using a 130 nm CMOS 3D Chartered/Tezzaron technology [3], featuring two layers bonded face-to-face. The top (outer) tier has been thinned down to less than 10 micrometres, while the bottom (inner) tier has not been modified with respect to the standard planar (2D) realization. The two tiers host two almost identical layouts featuring, among others, different matrices of 5×5 and 16×16 pixels. Each pixel is based on the standard three transistors (3T) active pixel architecture, featuring 10×10 micrometres area, with different sensitive element (photodiode) layouts. In particular, a *small* sensitive area with small capacitance aiming at maximizing the charge to voltage conversion gain (in the following simply referred as “small” for sake of concision) and a *large* sensitive area aiming at maximizing the fill-factor of the detector (in the following simply referred as “large” for the sake of concision) [2]. The structures of both tiers can be read-out in parallel by means of dedicated (separated) output bond pads, located at the backside of the top tier. The chip batches comprise a 2D version, a first 3D version (with a misaligned outer and inner tiers) and eventually a second 3D version featuring aligned tiers, obtained with two different bonding procedures, in the following referred as “Tezzaron aligned” and “Ziptronix aligned”.

In figure 1 are reported the schematic cross-sections of the different chip batches along with the corresponding micro-photographs of the real systems bonded on dedicated printed circuit test boards (PCB). From the 2D device top view (figure 1a) the chip structures are barely visible through the passivation layer, while in the case of both 3D devices (figures 1b — not aligned structures, and 1c — Tezzaron aligned structures) only the rear pads (to be used for the wire-bonding of the chip to the PCB) are visible. In particular, figure 1c refers to the chip fabricated with the Tezzaron [5] alignment procedure.

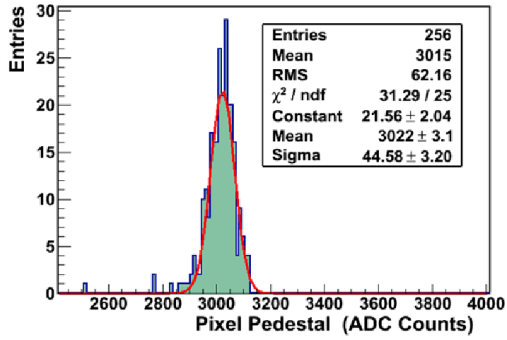


Figure 2. Large photodiode pedestal distribution.

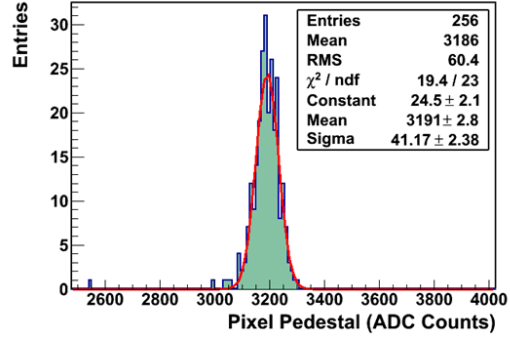


Figure 3. Small photodiode pedestal distribution.

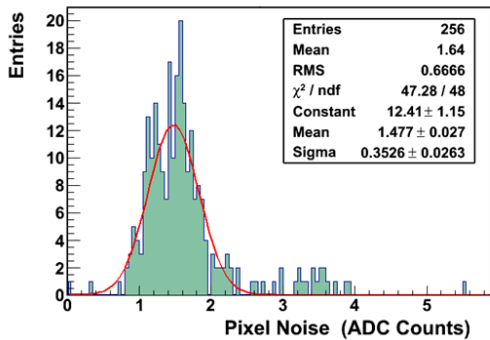


Figure 4. Large photodiode matrix noise evaluation.

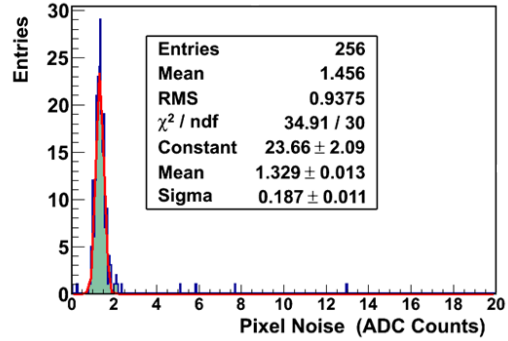


Figure 5. Small photodiode matrix noise evaluation.

2 System characterization

2.1 Electrical characterization

The electrical characterization of all structures has been carried out, in particular by looking at the pedestal and overall noise evaluation in dark conditions (e.g. when no external stimulus is applied). To begin with, the pedestal distributions of all pixels for the 16×16 matrix of 2D chips are reported in figures 2 and 3, for large and small photodiodes respectively. These figures are an indication of the uniformity of the whole matrix response in dark conditions, namely of the fixed pattern noise. By considering the standard deviation of these distributions, we decide to perform a pedestal subtraction procedure, in order to define the “baseline” of the signal to be compared with the output pixel signal when the hit occurs. The overall pixel noise evaluation has been therefore calculated by considering the standard deviation of the pixel signal distribution with respect to the pedestal subtracted mean value in dark condition, as reported in figures 4 and 5. The evaluated noise is around 1 ADC count, which is a good figure of merit if compared with typical signal amplitudes (see subsection 2.2 following).

In table 1 we report a summary of all the characterizations carried out on the different chips and different structures within the chips (outer and inner matrix layers), e.g. small and large diode matrices for the 2D structures (table on the top left), for the 3D not-aligned structures (table on the

Table 1. Mean pixel dark responses and corresponding standard deviations of all structures.

RAP504-2D					RAP504-3D Not Aligned				
#	Photodiode	σ (ADC)	μ (ADC)	T_{int} (μsec)	#	Photodiode	σ (ADC)	μ (ADC)	T_{int} (μsec)
1	Large	1.47	3022	512	1	Large OUT	1.04	3059	512
2					2	Large IN	0.91	3072	512
3	Small	1.32	3191	512	3	Small OUT	1.14	3021	512
4					4	Small IN	1.20	3067	512

RAP504-3D Aligned Tezzaron					RAP504-3D Aligned Ziptronix				
#	Photodiode	σ (ADC)	μ (ADC)	T_{int} (μsec)	#	Photodiode	σ (ADC)	μ (ADC)	T_{int} (μsec)
1	Large OUT	0.97	3014	512	1	Large OUT	0.94	3029	512
2	Large IN	0.82	3034	512	2	Large IN	0.81	3043	512
3	Small OUT	1.20	3021	512	3	Small OUT	1.12	3031	512
4	Small IN	1.21	3099	512	4	Small IN	1.28	3076	512

top right), and for both Tezzaron and Ziptronix 3D aligned structures (bottom tables). As a general remark, it should be pointed out that corresponding structures of the different 3D chips behave very similarly, not showing dependences on the bonding procedure, as expected.

2.2 Calibration

For sensor calibration purposes an Amptex Mini-X X-rays source has been used in fluorescence mode with different target materials, in particular Fe and Cu. The lines used for the calibration fit are the most abundant ones, typically K-alpha, which have been used to measure the response to photons of different energies (8.0 keV for Cu, 6.4 keV for Fe). With respect to figures 6 and 7, it should be noticed that the maximum amount of detected energy is the full incoming photon energy. The end points of the distributions are therefore good indicators of the maximum response. Each of these end points is defined by the convolution of the monochromatic energy with a Gaussian function typical of the sensor at hand. So the higher part of the spectrum is a Gaussian, and we can adapt the fitting in a way as to have this part well represented. The left part of the fit is not representing the spectrum due to the non-complete energy collection of the device, as typically seen for CMOS Monolithic Active Pixel sensors (see, e.g. [7] and [2]).

Given that, the mean value of the distribution does not depend very much on the selected data interval, as long as we reproduce well the end tail. Therefore, from the energy peak positions of Fe and Cu targets, the expected number of e/h pairs generated within the Si substrate can be estimated. The peak positions of the signal distributions correspond to an almost complete charge collection; therefore, a sensor calibration can be carried out, allowing an estimation of the conversion gain of around (25 ± 2) electrons per ADC for the small photodiode of the Tezzaron aligned structures and (24 ± 2) electrons per ADC for the Ziptronix aligned structures. No significant differences have been found between outer and inner tier structures. The conversion gain of the large photodiode structures was found of around (93 ± 17) electrons per ADC for the small photodiode of the Tezzaron aligned structures and (97 ± 17) electrons per ADC for the Ziptronix aligned structures. In this

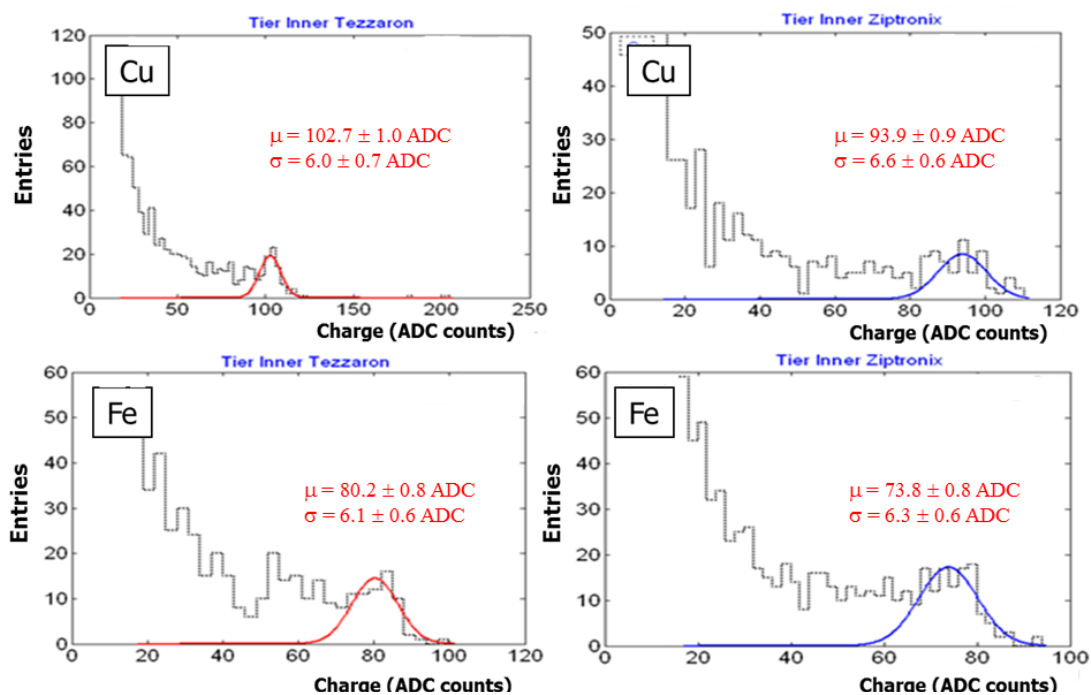


Figure 6. Responses of small photodiode matrices to 8.0 keV (Cu) and 6.4 keV (Fe) X-ray photons (inner layers).

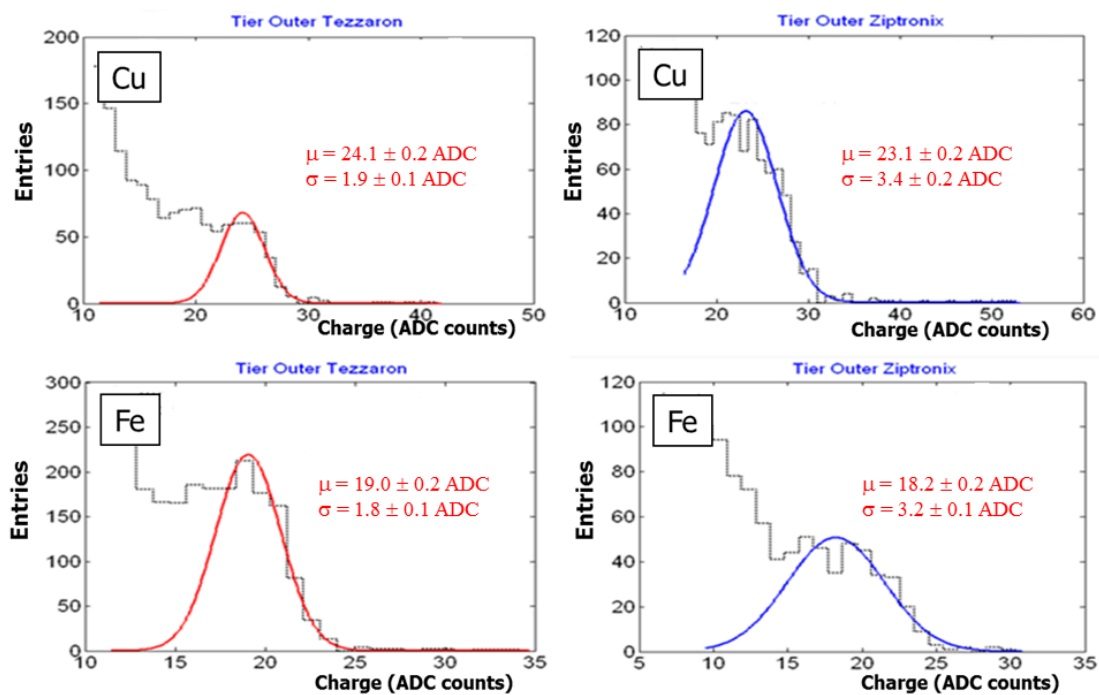


Figure 7. Responses of large photodiode matrices to 8.0 keV (Cu) and 6.4 keV (Fe) X-ray photons (inner layers).

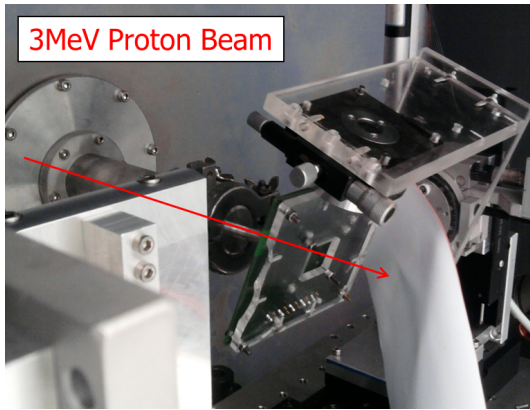


Figure 8. The test set-up at LABEC, Florence (Italy).

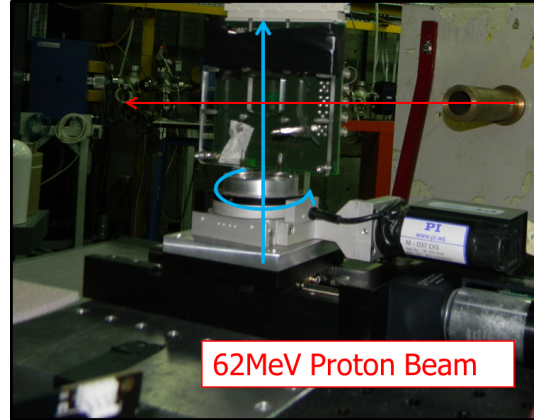


Figure 9. The test set-up at INFN LNS, Catania (Italy).

case too, all the corresponding structures of the two differently aligned 3D chip behave very similarly, and in agreement with the previous characterization carried out on not aligned structures [2].

3 Characterization with protons: angular measurements

In order to evaluate the suitability of the two layer monolithic active pixel sensor system to reconstruct particle tracks, tests with different energy proton beams have been carried out at the INFN LABEC laboratories in Florence, Italy with 3 MeV protons, and at the INFN LNS laboratories in Catania, Italy, with 62 MeV protons. The beam spot diameter is of the order of several squared millimetres, so the whole sensor undergoes a nearly uniform proton distribution, with an angular divergence of the order of few tens of milliradians, an order of magnitude less than the different angular positions used during the data taking. The set-ups are shown in figures 8 and 9; in both cases, the proton energy is sufficient to cross both outer and inner pixel layers, thus allowing the evaluation of the correlated responses.

Both not-aligned structures as well as aligned structures have been tested. Coincidence responses of the not aligned detectors showed a misalignment of more than 10 micrometres in both directions, as already pointed out [2].

The distributions of the residuals (namely, the differences between the coordinates of the impact points evaluated at the outer and inner layers) for both rows and columns with respect to an orthogonal beam incidence of 3 MeV protons are shown in figure 10. A Gaussian distribution with mean values of 1.08 pixel units for the x -axis (1 pixel unit = pitch = $10\ \mu\text{m}$) and 1.16 for the y -axis have been found. The additional peaks in the residual distribution are related to the quantized spatial differences, due to strictly mono-pixel responses which occur when a single pixel was hit.

A significantly different behaviour has been found when the aligned structures have been tested. Typical coincidence responses of outer and inner matrices are reported in figure 11. The plot of the residual distributions for both coordinates in this case for orthogonal beam incidence of 62 MeV protons shows an almost perfect alignment: residual mean values below 1 micrometre for both x -axis and y -axis coordinates have been found (figure 12).

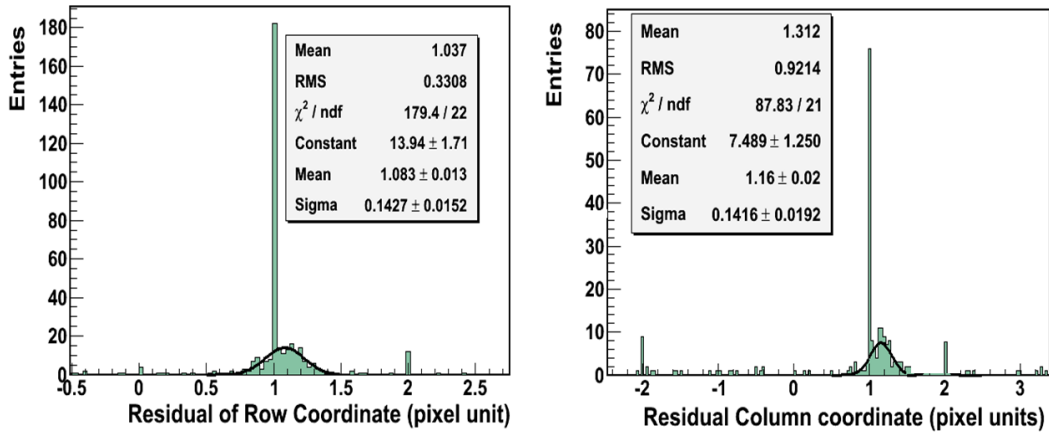


Figure 10. Residual distributions (e.g. differences between coordinates of the impact point evaluated on the outer and inner layers) for row and column coordinates for an orthogonal beam incidence (3 MeV protons).

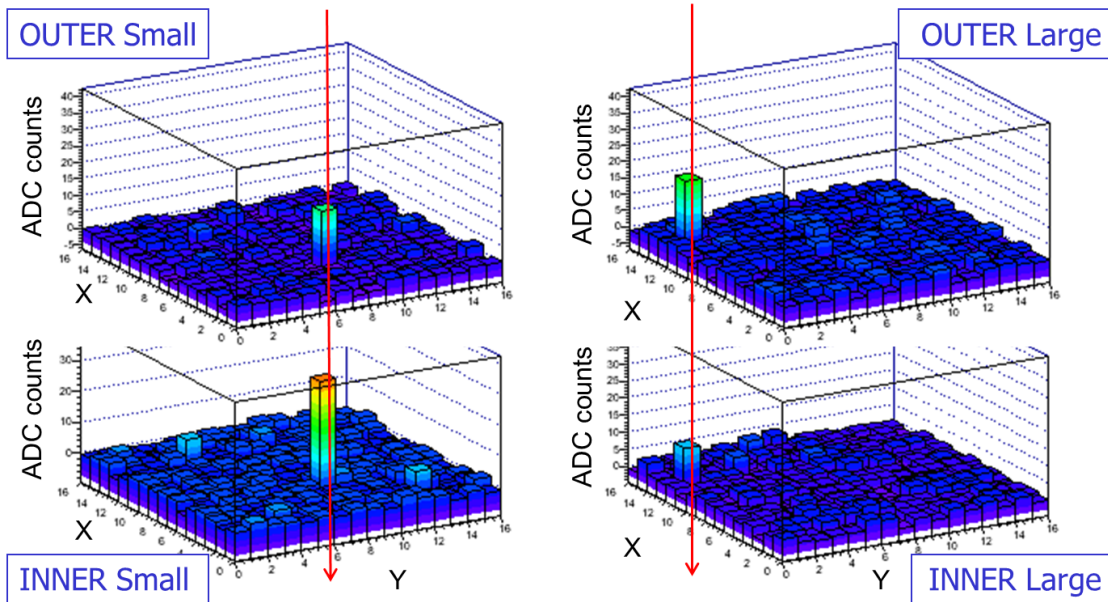


Figure 11. Responses of the outer and inner layer to the same hit (coincidence responses).

In order to check the suitability of the system for angular measurements, the chip has been tilted by steps of 1° with respect to the beam direction by means of the rotational stage. The residual distribution for the x -axis coordinates with respect to a rotation of the sensor around the y -axis are reported in figure 13. For orthogonal incidence, the residuals are located close to 0 as expected (some statistical fluctuations due to the noise are visible) while, for instance, for a 45° incidence angle a value of 1 pixel unit has been found. This is consistent with the relationship between the pixel pitch ($10 \mu\text{m}$) which is in the same order of the distance between the two layers of pixels. For increasing angle values, bigger differences between the coordinates measured on the inner and outer layers can be seen, as expected. At the same time, due to the more shallow

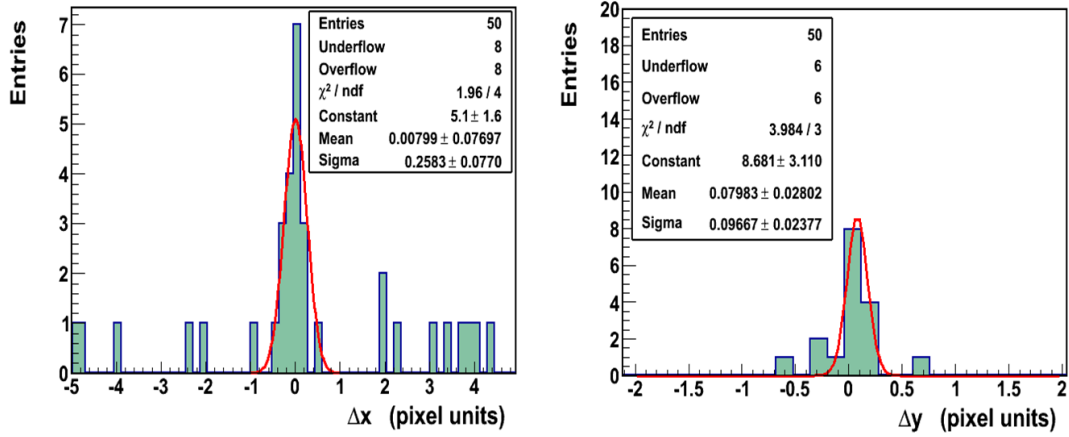


Figure 12. Residual distributions for aligned structures (orthogonal incidence of 62MeV protons).

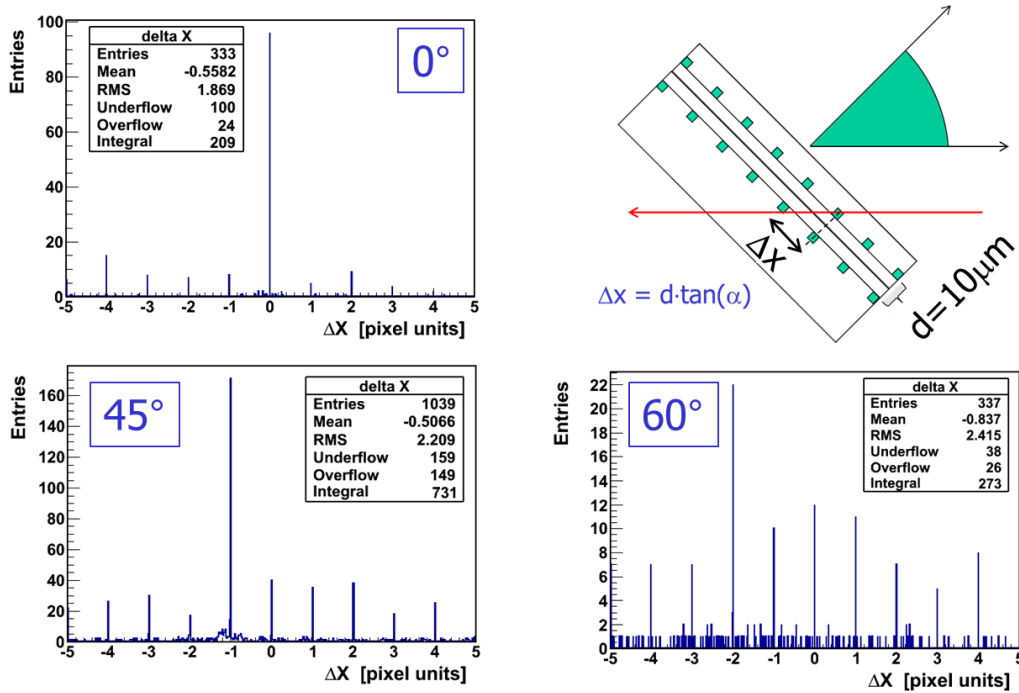


Figure 13. Residual distribution for the x -axis coordinates with respect to a rotation of the sensor.

generation between adjacent pixels (as a result of the grazing angle of the particle with respect to the detector plane) a “population” of the non discretize residual values due to charge sharing effects between pixels starts to become visible. The relatively low number of entries is due to the recording of a fixed amount of triggers for each different angular position, which have been selected with step of few degrees. Overflows and underflows are simply random coincidences, or some stray protons who deviate a lot from the beam line. Once again, due to the relatively low statistics, the reason of this effect can be only qualitatively explained.

4 Conclusions

A functional characterization of 3D monolithically stacked Active Pixel Sensor layers fabricated in Chartered/Tezzaron 130 nm 3D technology for particle tracking purposes has been carried out. Coincidence responses between bottom and top matrices have been obtained with 3 MeV and 62 MeV protons from aligned tiers. Particle angular measurement can be carried out by parallel reading of the corresponding outer and inner small pixel matrices. Particle direction measurement, fostering particle momentum evaluation, with a single, multiple layers, 3D vertically stacked APS CMOS detector would be therefore possible.

References

- [1] D. Passeri, L. Servoli and S. Meroli, *Analysis of 3D stacked fully functional CMOS Active Pixel Sensor detectors*, 2009 *JINST* **4** P04009.
- [2] D. Passeri et al., *3D monolithically stacked CMOS active pixel sensor detectors for particle tracking applications*, 2012 *JINST* **7** C08008.
- [3] CMS collaboration, *Conceptual study of a trigger module for the CMS Tracker at SLHC*, *Nucl. Instrum. Meth. A* **636** (2011) 201.
- [4] 3DIC Consortium <http://3dic.fnal.gov/>.
- [5] <http://www.tezzaron.com/technology/technology.html>.
- [6] D. Biagetti et al., *CMOS Active Pixel Sensors for soft X-rays detection applications*, *IEEE Nucl. Sci. Symp. Conf. Rec.* **2008** (2008) 3459.
- [7] L. Servoli, D. Biagetti, D. Passeri and E. Spanti Gattuso, *Characterization of standard CMOS pixel imagers as ionizing radiation detectors*, 2010 *JINST* **5** P07003.